DR-1680
U-36

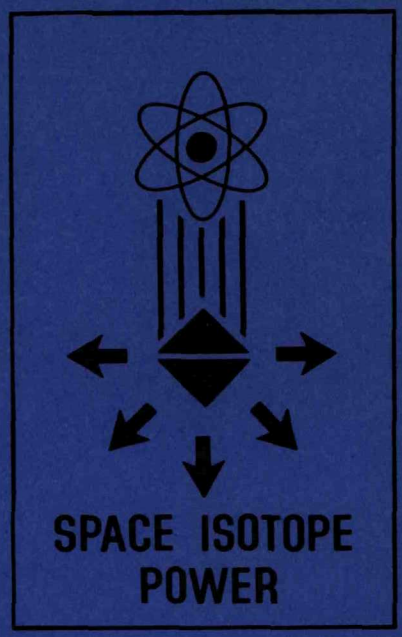

SC-RR-70-804

A STUDY OF THE EFFECT OF THE EVAPORATIVE EROSION ON THERMOELECTRIC ELEMENTS ON THE PERFORMANCE OF THERMOELECTRIC GENERATORS

RAGON D. KINNEY,
Space Power Advanced Development Division

Published - November 1970

SANDIA LABORATORIES

OPERATED FOR THE UNITED STATES ATOMIC ENERGY COMMISSION BY SANDIA CORPORATION | ALBUQUERQUE, NEW MEXICO, LIVERMORE, CALIFORNIA

DISCLAIMER

Issued by Sandia Corporation,
a prime contractor to the United States Atomic Energy Commission

---

Available from the Clearinghouse
U. S. Department of Commerce,
Springfield, Virginia 22151

Price: Paper Copy $3.00
Microfiche $0.65

SC-RR-70-804

A STUDY OF THE EFFECT OF THE EVAPORATIVE EROSION ON THERMOELECTRIC ELEMENTS ON THE PERFORMANCE OF THERMOELECTRIC GENERATORS

Ragon D. Kinney, 9522
Space Power Advanced Development Division
Sandia Laboratories
Albuquerque, New Mexico
87115

November 1970

ABSTRACT

A model is presented and an analysis made of the material losses from thermoelectric elements in some thermoelectric generators and the effect of such loss on generator performance.

Key Words: PbTe, vapor transport

ACKNOWLEDGMENT

The author wishes to acknowledge the assistance of Ivan Waddoups during this study; specifically, his effort in the use of the computer codes.

TABLE OF CONTENTS

BLANK

A STUDY OF THE EFFECT OF THE EVAPORATIVE EROSION ON THERMOELECTRIC ELEMENTS ON THE PERFORMANCE OF THERMOELECTRIC GENERATORS

Introduction

A mode of performance degradation in some thermoelectric generators is the erosion of material from the thermoelectric elements that comprise the generator. In pressurized generators using an inert gas to retard sublimation of the thermoelectric material, this erosion results from diffusive mass transport of vapor from the elements due to naturally occurring concentration gradients in the surrounding cover gas. The erosion occurs primarily at the hot end of the elements and diminishes the area of contact between the element and its electrical connection. This report presents an analysis of the effect erosion has on generator performance.

Model Description

Figure 1 depicts a longitudinal section of the configuration chosen for analysis, i.e., one element of a thermoelectric couple, typically a PbTe couple, surrounded by thermal insulation. Referring to this figure, the annular region between the cylindrical PbTe thermoelectric element and the surrounding thermal insulation is gas filled, and as a result of the element residing in the temperature gradient, $(T_h - T_c)/\ell$, concentration gradients of PbTe vapor exists in the annular region. These gradients promote the diffusion of material through the cover gas away from the hot end of the element, $z = 0$. Steady state equilibrium is supported by material subliming from the element to replace that which diffuses away. Hence, the element erodes.

The configuration of Figure 1 represents well only those generator designs, such as the SNAP-19, which use a molded insulation around the thermoelectric element and have a relatively uniform gas filled annular region. However, the

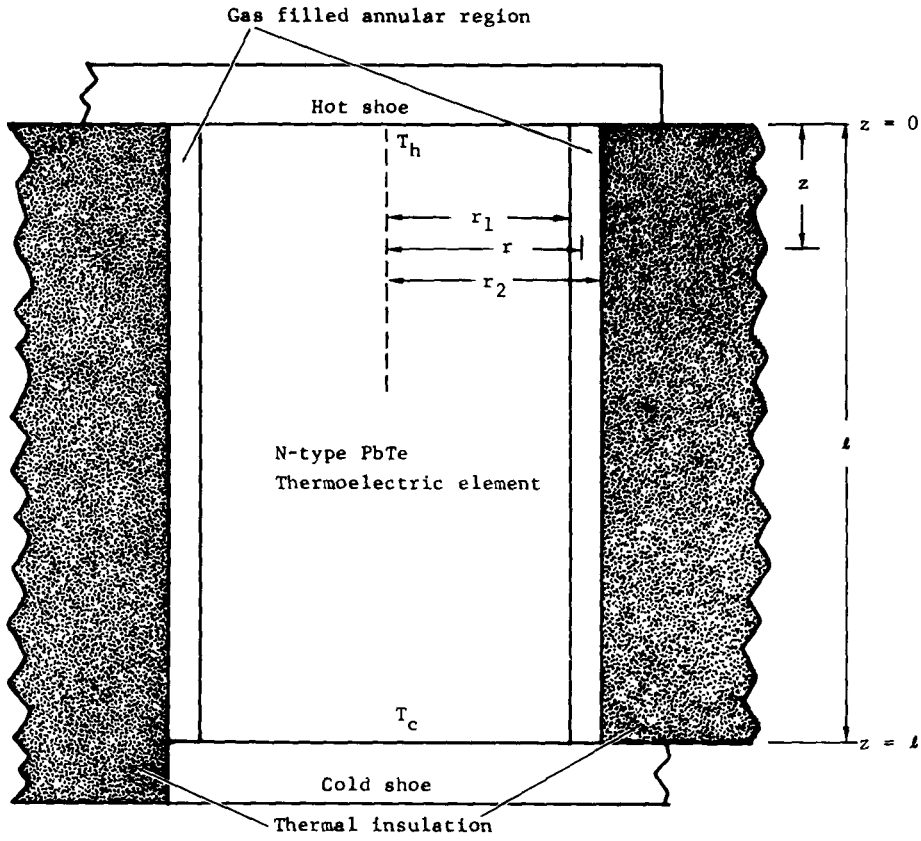

Figure 1. Configuration of thermoelectric element and thermal insulation used for analysis

general trends revealed by the analysis can apply to more irregular geometries such as might occur on the SNAP-27 where the insulation has been powdered and lightly tamped around the thermoelectric elements, but where diffusion through the cover gas remains the dominant mode of mass transport.

Determining the deviation in total generator performance due to element erosion is accomplished by first developing an expression for predicting the contour of the thermoelectric element after time, t, and secondly by using this information in thermoelectric generator computer design codes to assess the performance of couples with eroded elements relative to their performance with whole elements.

An expression for the profile history of the thermoelectric element depicted in Figure 1 is developed by considering the time rate of change in the radius of the element due to erosion. This is given as

$$dr/dt = - j_{r_1}/\rho \tag{1}$$

where

r = radius of the thermoelectric element

j_{r_1} = steady state radial component of mass flux at the surface of the element, i.e., mass flux evaluated at $r = r_1$.

ρ = density of thermoelectric material

Assuming the mass transport due to temperature gradients and bulk motion of the cover gas is negligible, and the total system pressure is spatially constant, the general form of the radial component of mass flux, j_r, can be expressed as

$$j_r = \frac{C(m,t)}{P} \partial p_1/\partial r \text{ gm} \cdot \text{cm}^{-2} \cdot \text{sec}^{-1} \tag{2}$$

where

$C(m,t)$ = constant depending on the gas species and temperature, $gm \cdot cm^{-1} \cdot sec^{-1}$

p_1 = partial pressure of the vapor of the thermoelectric material, atmospheres.

P = total pressure in system, atmospheres

A complete development for the constant, $C(m,t)$, can be found in a previous report[1] by the author on this subject.

Neglecting the slight spatial dependence of $C(m,t)$ in Equation (2) and solving Laplace's equation for p_1 for the particular geometry of Figure 1 will give the required expression for j_r. In other words, one must determine a solution to the following equation for appropriate boundary conditions,

$$\partial^2 p_1 / \partial r^2 + \frac{1}{r} \partial p_1 / \partial r + \partial^2 p_1 / \partial z^2 = 0 \qquad (3)$$

where

r = radial coordinate of Figure 1

z = axial coordinate of Figure 1

The expression for p_1 which satisfies Equation (3) is then used in Equation (2). The boundary conditions best describing the environment of the couple in Figure 1 are:

(1) $\partial p_1 / \partial r = 0$ at $r = r_2$

(2) $\partial p_1 / \partial z = 0$ at $z = 0$

(3) $p_1 = 0$ at $z = \ell$

(4) $p_1 = f(z)$ at $r = r_1$ where $f(z)$ is the equilibrium vapor pressure of the thermoelectric material along the surface of the element.

Model Solution

The solution of Equation (3) for the preceding boundary conditions is

$$p_1 = \frac{2}{\ell}\sum_{n=1}^{\infty} \frac{F(\lambda_n r_2;\lambda_n r)}{F(\lambda_n r_2;\lambda_n r_1)} \cos \lambda_n z \int_o^{\ell} f(z) \cos \lambda_n z \, dz \qquad (4)$$

where

$$F(x;y) = I_1(x)K_o(y) + K_1(x)I_o(y)$$

I_ν = modified Bessel function of the first kind of order ν

K_ν = modified Bessel function of the second kind of order ν

ℓ = length of annular segment depicted in Figure 1

$\lambda_n = (2\,n - 1)\,\pi / 2\ell$

The function, f(z), generally has the form

$$f(z) = A \exp\,[-B/T(z)] \qquad (5)$$

where

A and B are constants of the thermoelectric material

T(z) = surface temperature along axial coordinate of the element, °K

Assuming the distribution of temperature along the surface of the thermoelectric element is linear, T becomes

$$T = T_h - (T_h - T_c)\, z/\ell \qquad (6)$$

where

T_h = thermoelectric element hot junction temperature, °K

T_c = thermoelectric element cold junction temperature, °K

Substitution of Equation (5) and (6) into Equation (4) completes the solution of p_1. For this analysis,

$$A = \exp(16.23)$$

$$B = 25.97 \times 10^3$$

which are values taken from work by D. Northrup[2]. A more complete discussion of the above developments can be found in Reference (1)

Assuming the series expression for p_1 as given in Equation (4) converges uniformly, the partial derivative, $\partial p_1/\partial r$, and thus j_r can be numerically evaluated for values of the dimensionless variables r/ℓ and z/ℓ, with the exception of the point ($z = 0$, $r = r_1$) which, in this case, is the intersection of two incompatible boundary conditions, (2) and (4). Figure 2 plots $\partial p_1/\partial r$ at $r = r_1$ as a function of z/ℓ for a typical set of parameters. For example, the parameters $r_1/\ell = 0.380$ and $r_2/\ell = 0.580$ of Figure 2 would be representative of a cylindrical thermoelectric element of 0.380" diameter and 0.500" length separated from the surrounding insulation by an annular gap of 0.100 inch.

Using an expression from Reference (1) to evaluate C(m, t) of Equation (2) for a mixture of Argon gas and PbTe vapor at T = 600°C gives

$$C(m, t) = 0.0019 \text{ gm} \cdot \text{cm}^{-1} \cdot \text{sec}^{-1}$$

This value of C(m, t) and the values of $\partial p_1/\partial r$ from Figure 2 defines j_{r_1} (for the above parameters) for various pressures of cover gas. Assume, for the following analysis, that the generated pressure is constant with time. Substituting Equation (2) for $r = r_1$ into Equation (1) and integrating will give

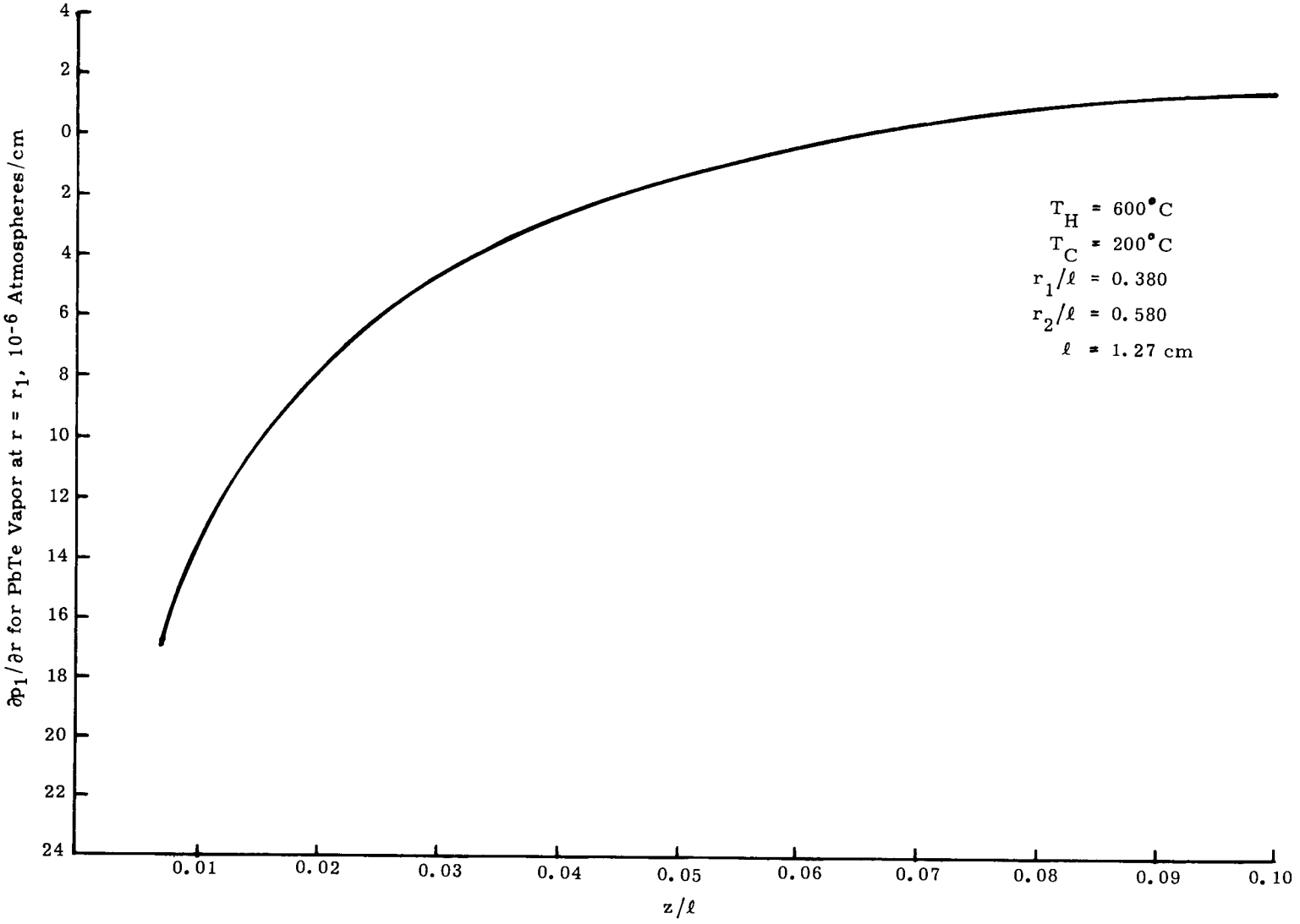

Figure 2. Partial pressure gradient of PbTe vapor near z = 0

$$r = r_o - j_{r_1} t/p \tag{7}$$

where

r_o = initial radius of thermoelectric element, cm

t = time, sec

ρ = density of thermoelectric material, gm · cm^{-3}

Figure 3 shows the profile, after one year, of a PbTe thermoelectric element as calculated from Equation (7) for one atmosphere generator pressure of Argon and the configuration parameters stated in Figure 2. Values of j_{r_1} near $z = 0$ were determined by evaluating $\partial p_1/\partial r$ for points in the annular region slightly outside the boundary, r_1, where the discontinuity at $z = 0$ could be avoided. Note the rounding of element near the hot end due to diffusion of material away from the element. The element also shows a region of material deposition immediately below the eroded section. Almost all of the redistribution of material occurs within the first 40 to 50 percent of the element. The profile of Figure 3 is typical of the deterioration resulting from the particular configuration and boundary conditions of Figure 1. Increasing or decreasing the boundary r_2 of Figure 1 respectively increases and decreases the partial pressure gradients, $\partial p_1/\partial r$, and thus the severity of erosion; but the shape of the element remains generally the same.

Couple Behavioral Analysis

Initial speculation on the effect of erosion on generator performance suggested that for constant heat input, the hot junction temperature would rise due to increase in thermal resistance of each element and the power output would decrease due to increases in electrical resistance. This prediction was essentially correct. This was shown by comparing the temperatures and power outputs of whole couples with eroded couples as calculated by a computer design code, VINCE TOM-MOD. 1.

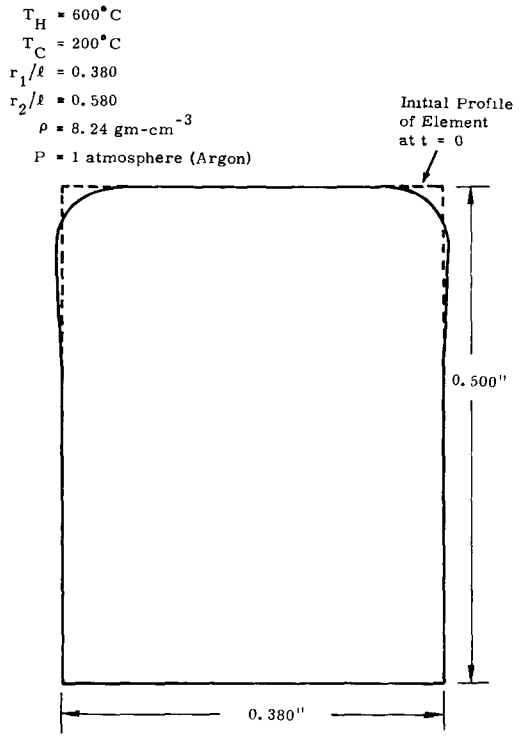

Figure 3. Profile of thermoelectric element showing erosion after one year

This code was originally developed by Martin Marietta, Inc. and is unique, in at least one feature, in allowing variable cross sectional areas for the elements. Using this code, the power outputs and hot junction temperatures of eroded couples were determined for constant heat input and cold junction temperature. Figure 4 shows the plots, for selected intervals of time, of a normalized power output for ten couples, i. e., the ratio of power output of the couples to their initial power; and the hot junction temperature. The power output in early life appears to be dictated by the combination of increasing hot junction temperature and electrical resistance. In later life, the behavior is dominated by the rapid increase in electrical resistance of the couples due to the advanced state of erosion. It is interesting that for the particular parameters stated in Figure 4, this model predicts zero area for the "P" elements at their hot end contacts within approximately 2 years for P = 1 atmosphere.

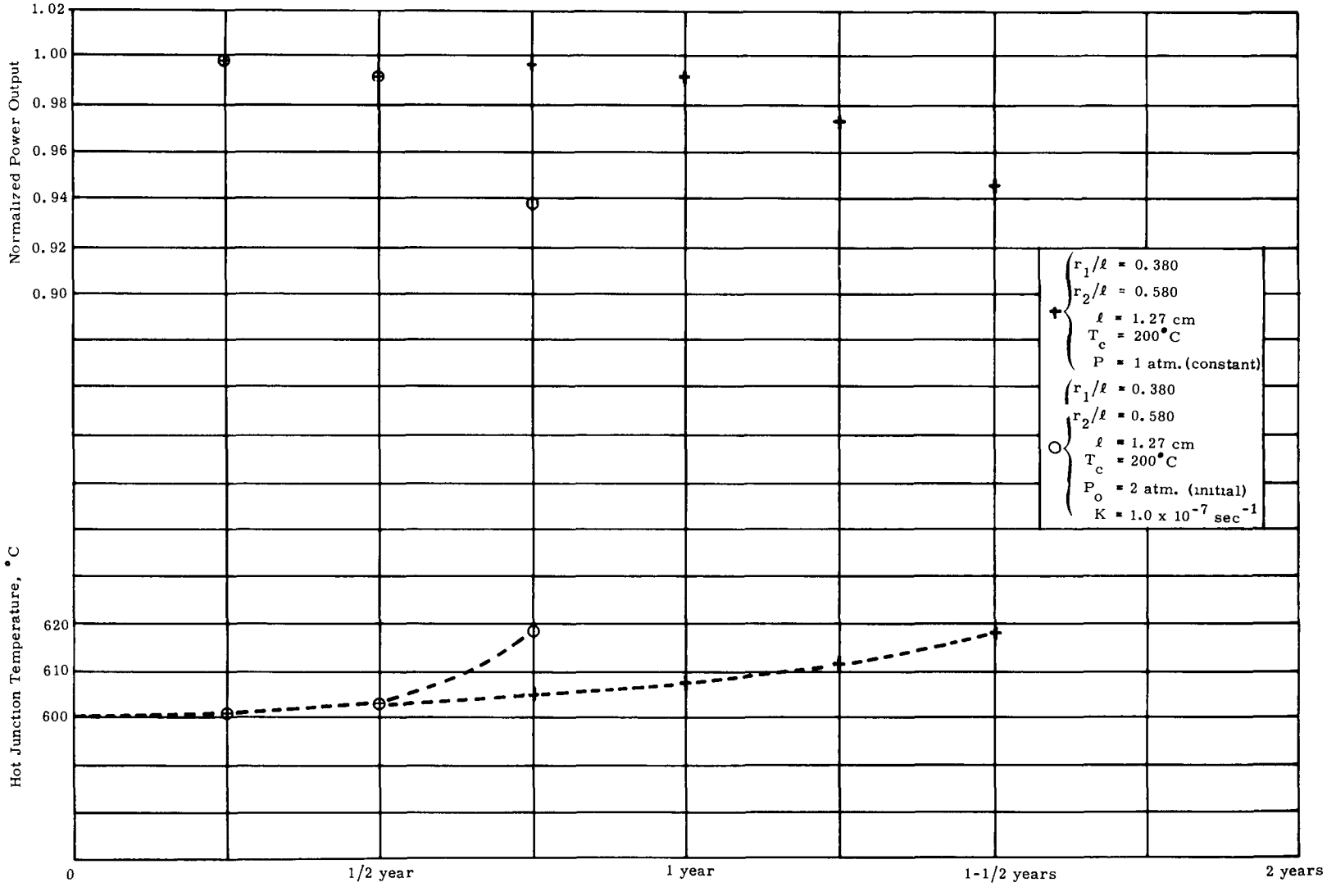

Figure 4. Performance history of thermoelectric couples showing effect of erosion

In addition to the analysis in which the generator pressure was held constant in time, an analysis was made which allows for pressure decay as a function of time. This condition would be present in most gas filled generators operating in space. For this case, the generator pressure, P, in Equation (2) was assumed to be of the form

$$P = P_o e^{-Kt} \text{ atmospheres} \tag{8}$$

where

P_o = initial generator pressure, atmospheres

K = constant depending on the leak rate and volume of generator, sec^{-1}

t = time, sec

Substitution of Equation (8) into j_{r_1} of Equation (1) and integrating results in

$$r = r_o - j_{r_1}(P_o)\,(e^{Kt} - 1)/\rho K \tag{9}$$

where $j_{r_1}(P_o)$ is j_{r_1} evaluated for the initial pressure, P_o. This derivation assumes that the slow loss of generator pressure does not perturb the steady state equilibrium of the gas system. Equation (9) can be used in the same fashion as Equation (7) to calculate the radius and hence the cross section area of the thermoelectric elements as a function of time. Figure 4 shows couple performance for this condition as calculated by the aforementioned computer code, VINCE TOM-MOD. 1. Note that for P_o = 2 atmospheres of Argon and K = 1.0×10^{-7} sec^{-1}, the resulting deterioration in couple performance occurs earlier for the same configuration parameters, r_1/ℓ and r_2/ℓ, than in the preceding case. For the present case, the occurrence of zero contact area for the "P" element occurred at about 0.8 year as compared to 2 years for the constant pressure case.

Model Limitations

There are several deficiencies in the model that should be mentioned. The above analyses predicted complete erosion of the "P" elements at their hot end contacts. For spring loaded couples this is not realistic since the spring loading will keep the shortened element in contact with the hot shoe for a much longer period. However, this condition was not studied, and due to this uncertainty in couple behavior for severe erosion, only the first portion of the performance histories are plotted in Figure 4.

No account was taken of the increase in material loss that will occur due to the increases in hot junction temperature. Since the material flux, j_r, is highly dependent on temperature, this increase, even for small changes, may be significant.

This model, p_1, assumes in the solution for the partial pressure distribution a constant boundary, $r = r_1$, with time. This, of course, is not the case. However, the changes in p_1 and j_{r_1} due to boundary changes is not likely to be of such significance as to change the conclusions of this analysis.

Conclusions

The preceding study, based on the model described, shows that there can be material loss from thermoelectric elements even in generators using a cover gas. This erosion of the elements could cause a significant portion of the degradation observed in current thermoelectric generators. It is, however, not of such magnitude to account for all of the degradation.

REFERENCES

1. Kinney, R. D., The Evaporative Erosion of Thermoelectric Elements in Some Thermoelectric Generators, SC-RR-70-534, Sandia Laboratories, Albuquerque, New Mexico, September 1970 (U).

2. Northrop, D. A., Vaporization of Some Commercial Telluride Thermoelements, SC-TM-68-500, Sandia Laboratories, Albuquerque, New Mexico, July 1968.

DISTRIBUTION:

TID-4500 (56th Ed.) UC-36 (150)

U. S. Atomic Energy Commission (5)
Division of Space Nuclear Systems
Space Electric Power Office
Washington, D. C. 20545
Attn: G. A. Newby
Assistant Director
G. P. Dix, Chief
Safety Branch
R. T. Carpenter, Chief
Isotope Power Sys. Branch
J. A. Powers, Chief
Isotopes Fuels and Matls. Br.
C. E. Johnson, Chief
Reactor Power Sys. Branch

U. S. Atomic Energy Commission
Space Nuclear Propulsion Office
Washington, D. C. 40545
Attn: R. S. Decker, Jr., Chief
Safety Branch

U. S. Atomic Energy Commission
Division of Isotope Development
Washington, D. C. 20545

U. S. Atomic Energy Commission (2)
Director of Regulation
Washington, D. C. 20545
Attn: C. K. Beck
Deputy Director
R. W. Klecker
Div. of Reactor Licensing

U. S. Atomic Energy Commission (2)
Division of Biology and Medicine
Washington, D. C. 20545
Attn: J. Z. Holland
Fallout Studies Branch
H. D. Bruner, Asst. Dir.
Medical and Health Research

U. S. Atomic Energy Commission
Space Nuclear Propulsion Office
Albuquerque Extension
Albuquerque Operations Office
P. O. Box 5400
Albuquerque, New Mexico 87115
Attn: H. P. Smith

U. S. Atomic Energy Commission (2)
Albuquerque Operations Office
P. O. Box 5400
Albuquerque, New Mexico 87115
Attn: B. W. Colston, Director
Space and Special
Projects Division
For: J. Nicks
J. F. Burke, Director
Operational Safety Div.

AEC Site Representative
National Aeronautics and Space Adm.
Manned Spacecraft Center
Houston, Texas 77058
Attn: W. C. Rémini
Bldg. 16, Code ZS-5

Deputy I. G. for Insp. & Safety
USAF
Directorate of Nuclear Safety
Nuclear Power Division
Kirtland Air Force Base
New Mexico 87117

Jet Propulsion Laboratory
California Institute of Technology
4800 Oak Grove Drive
Pasadena, California 91103
Attn: A. L. Klascius
Radiation Health and Safety

Los Alamos Scientific Laboratory (5)
P. O. Box 1663
Los Alamos, New Mexico 87544
Attn: Dr. L. D. P. King
Dr. Wright Langham
C. F. Metz, CMB-1
F. W. Schonfeld, CMF-5
J. A. Leary, CMB-11

Monsanto Research Corporation
Mound Laboratory
P. O. Box 32
Miamisburg, Ohio 45342
Attn: G. R. Grove

Thomas B. Kerr
Code RNS
National Aeronautics and Space Adm.
Washington, D. C. 20545

DISTRIBUTION: (cont)

Mr. Glenn Goodwin
National Aeronautics and Space Adm.
Ames Research Center
N-200-4
Moffett Field, California 94035

National Aeronautics and Space Adm.
Goddard Space Flight Center
Glenn Dale Road
Greenbelt, Maryland 20771
Attn: A. W. Fihelly
Nimbus Project

Naval Facilities Engineering Com.
Dept. of the Navy, Code 042
Washington, D. C. 20390

Space Nuclear Propulsion Office
Lewis Research Center
21000 Brookpark Road
Cleveland, Ohio 44135
Attn: L. Nichols

Mr. George Mandel
Information Specialist
Aerospace Safety Research and
Data Institute
NASA Lewis Research Center
21000 Brookpark Road
Cleveland, Ohio 44135

Union Carbide Corporation (2)
Nuclear Division
P. O. Box X
Oak Ridge, Tennessee 37831
Attn: R. A. Robinson
Isotope Development Center
B. R. Fish
Health Physics Division

U. S. Public Health Service
Nat. Ctr. for Radiological Health
1901 Chapman Avenue
Rockville, Maryland 20852
Attn: Nuclear Facilities Section

D. B. Shuster, 1200
J. R. Holland, 5321
C. F. Bild, 7500
G. A. Fowler, 9000
J. R. Banister, 9150
R. C. Maydew, 9320
L. A. Hopkins, Jr., 9500
A. J. Clark, Jr., 9510
S. L. Jeffers, 9512
ARPIC, 9512 (2)
S. McAlees, Jr., 9513
G. J. Hildebrandt, 9520
G. J. Hildebrandt, 9521 (Actg)
J. Jacobs, 9522
Central Files, 3422-1 (15)
L. C. Baldwin, 3412
L. L. Alpaugh, 3412
G. C. McDonald, 3416 (3)